ISSN: 0067-2904

Synthesis and Evaluation of 3-(4-bromobenzyl)-2-mercaptoquinazolin-4(3H)-one as a Corrosion Inhibitor for carbon steel CS45 in 1M HCl

Esraa Ali Arrak*, Oday H. R. Al-Jeilawi
Department of Chemistry, College of Science, University of Baghdad, Jadriyah, Baghdad 10011, Iraq.

Received: 10/3/2025 Accepted: 29/ 5/2025 Published: 30/5/2026

Abstract:

In this study, a mercapto-quinazolinone derivative, 3-(4-Bromobenzyl)-2-mercaptoquinazolin-4(3H)-one (compound B), was synthesized and assessed as a corrosion inhibitor for carbon steel (CS45) in 1M hydrochloric acid. The synthesis began with anthranilic acid and involved two main steps: first, the formation of a thiocyanate intermediate, followed by its reaction with anthranilic acid to produce compound B. The chemical structure of the synthesized compound was confirmed using FT-IR, ^{1}H-NMR, and ^{13}C-NMR techniques. The corrosion inhibition performance of compound B was evaluated at different concentrations (0.01, 0.05, 0.1, and 0.3 M) and temperatures (293, 303, and 313 K) in acidic media. Potentiodynamic polarization measurements indicated that compound B is an effective corrosion inhibitor, achieving a maximum inhibition efficiency of 96% at a concentration of 0.3 M and a temperature of 293 K. Additionally, the results showed a relationship between inhibitor concentration and current density, demonstrating that increasing the inhibitor concentration led to a decrease in current density. The study also showed that the inhibitor follows the Langmuir rule for adsorption and that compound B is a mixed inhibitor

Keywords: Thiocyanate derivative ; Quinazolinone derivative ; Corrosion inhibition; Inhibition efficiency ; Factors influencing corrosion (temperature and concentration); Potentiostat; Tafel slopes.

تحضير وتقييم مركب 3-(4-بروموبنزايل)-2-مركبتوكوينازولين-4(3H)-اون كمثبط تآكل للفولاذ الكربوني CS45 في حامض الهيدروكلوريك 1مولاري

اسراء علي عراك* ، عدي هادي رؤوف الجيلاوي
قسم الكيمياء، كلية العلوم، جامعة بغداد، الجادرية، بغداد 10011، العراق

الخلاصة

في هذه الدراسة تم تحضير مشتق مركبتو-كوينازولينون (3-(4-بروموبنزايل)-2-مركبتوكوينازولين-4(3H)-اون) (المركب B) و تقييمه كمثبط تآكل للفولاذ الكربوني (CS45) في حامض الهيدروكلوريك 1 مولاري. بدأ التحضير بحامض الأنثرانيليك و شمل خطوتين رئيسيتين: اولاً، تكوين وسيط الثايوسيانات, يليه تفاعله مع حامض الأنثرانيليك لإنتاج المركبB. تم تأكيد التركيب الكيميائي للمركب المحضر باستخدام

*Email: israa.arak2305@sc.uobaghdad.edu.iq

تقنيات FT–IR، ^{1}H–NMR و^{13}C–NMR. قُيم اداء المركب B في تثبيط التاكل عند تراكيز مختلفة (0.01,0.05,0.1,0.3) مولاري و
درجات حرارة (293، 303، 313 كلفن) في اوساط حامضية. اشارت قياسات الاستقطاب الديناميكي الى ان المركب B مثبط تآكل فعال، حيث حقق اقصى كفاءة للتثبيط بنسبة 96٪ عند تركيز 0.3 مولاري ودرجة حرارة 293 كلفن. بالاضافة الى ذلك , اظهرت النتائج وجود علاقة بين تركيز المثبط وكثافة التيار، مما يدل على أن زيادة تركيز المثبط تؤدي الى انخفاض في كثافة التيار. كما اظهرت الدراسة ان المثبط يتبع قاعدة لنكماير للامتزاز, وان المركب B مثبط مختلط.

1. Introduction

Mild steel, an iron (Fe) alloy known for its mechanical durability, is the most widely utilized type of steel. Its popularity in industry because of its low production cost and ease of processing. However, when steel is exposed to processes such as acid pickling, industrial washing, acid descaling, and oil-wet cleaning, mild steel is prone to corrosion, leading to substantial economic losses [1, 2]. The use of inhibitors is one of the most effective and economical methods for preventing corrosion. These corrosion inhibitors often contain functional groups such as oxygen (O), nitrogen (N), phosphorus (P), and sulfur (S), as well as aromatic and heterocyclic rings [3]. Different environments exhibit varying levels of corrosiveness. While there are exceptions, the following claims are widely acknowledged: compared to dry air, moist air is more corrosive; hot air is more corrosive than cold air; Polluted air is more corrosive than clean air; hot water is more corrosive than cold water; fresh water with low chloride content is less corrosive than salt water; acids corrode steel more than bases (alkalis); and stainless steel (SS) resists corrosion better than regular steel. Additionally, even at extremely high temperatures, there is no corrosion in a vacuum [4]. One of the important applications of quinazolinone derivatives is their use as corrosion inhibitors in various acidic environments[5] . They are selected as corrosion inhibitors because they contain heteroatoms, aromatic rings, and functional groups, which impart strong anti-corrosion properties[6, 7]. These corrosion inhibitors readily adsorb onto metal surfaces[8]. Moreover, most organic compounds contain functional groups such as a coordinated bonds, aromatic structures[9], or other electron-donating centers, which enhance their ability to prevent corrosion [10]. Despite the low cost and mechanical strength of carbon steel, it is prone to corrosion when exposed to corrosive environments [11, 12]. The deterioration of metals and alloys due to corrosion results in significant economic losses, with billions of dollars spent annually to mitigate the problem [13, 14]. While it is impossible to entirely prevent corrosion [15, 16], corrosion inhibitors continue to be among the most effective approaches for protecting metal surfaces [17].Quinazolinone derivatives are organic compounds that feature a heterocyclic structure containing nitrogen and oxygen atoms. These atoms play a key role in the ability of quinazolinone derivatives to adsorb onto metal surfaces, forming a protective barrier that prevents corrosion. The nitrogen atoms, in particular, can form coordinate bonds with metal atoms, enhancing the inhibitor's ability to passivate the metal surface, thereby reducing the rate of electrochemical reactions responsible for corrosion [18]. Research has demonstrated the efficiency of quinazolinone derivatives as corrosion inhibitors for a variety of metals, including mild steel, copper, and aluminum alloys. These compounds show significant inhibition of corrosion, particularly in acidic environments like sulfuric acid and hydrochloric acid solutions, commonly used in industrial applications such as cleaning, pickling, and oil field operations [19]. This study focuses on evaluating quinazolinone derivatives as corrosion inhibitors for metals in acidic environments. Experimental investigations, utilizing electrochemical and weight loss methods, revealed that compound B achieved an inhibition efficiency of 96% at a concentration of 0.3 M when used to protect carbon steel in 1 M hydrochloric acid.

2. Experiments

2.1 *Materials and Methods*

All materials and solvents used in this study were supplied from BDH, Fluka, and Sigma-Aldrich. A Gallenkamp capillary melting point apparatus was used to determine melting points. Thin-layer chromatography (TLC) was performed using silica gel to monitor reaction progress, with a solvent system of ethyl acetate: petroleum ether (1:2). TLC plates were visualized under ultraviolet (UV) light to detect spots. FT-IR spectra were recorded using a Shimadzu FT-IR8400 Fourier Transform Infrared spectrophotometer with KBr disc. Nuclear magnetic resonance (NMR) spectra were obtained using a BRUKER spectrometer operating at 300 MHz for ^{1}H-NMR and 75 MHz for ^{13}C-NMR, with acetone-d_6 as the solvent and tetramethylsilane (TMS) as the internal standard.

2.2.1. *Synthesis of P-Bromo Benzyl Thiocyanate (A)* [20, 21].

Potassium thiocyanate (KSCN, 0.01 mol, 0.97 g) was dissolved in anhydrous acetone (10 mL). Then, p-bromobenzyl chloride (0.01 mol, 2.05 g) was added to the solution. The reaction mixture was stirring for 30 minutes. Reaction progress was monitored by thin-layer chromatography (TLC) using a mobile phase of petroleum ether: ethyl acetate (2:1, v/v). After completion of the reaction, the product was filtered to remove the potassium chloride salt. The filtrate was poured onto crushed ice to induce precipitation. The precipitated compound was filtered and dried. TLC analysis confirmed that the compound was a pure single substance.

Pale-yellow solid; Chemical formula C_8H_6NOSBr ; yield: 95%; m.p. 73–75°C ;R_f=0.73 ; FT-IR (υ, cm^{-1}): 3090 (C-H $_{aromatic}$) ; 2917,2850(C-H $_{aliphatic}$); 2152(N=C=S) ; 1517 (C=C aromatic) ; 858 (C-Br).

2.2.2. *Synthesis of 3-(4-Bromobenzyl)-2-mercaptoquinazolin-4(3H)-one (B)* [22, 23].

A mixture of anthranilic acid (0.01 mol, 1.37 g) was mixed with thiocyanate derivative (A) (0.01 mol, 2.279 g), followed by the addition of triethylamine (0.01 mol, 1.39 mL) to the mixture in 10 mL of anhydrous acetone. The reaction mixture was refluxed for 5 hours, with progress monitored by thin-layer chromatography (TLC). Upon completion, the reaction mixture was poured over crushed ice to induce precipitation of the product. The precipitate was filtered, washed multiple times with ethanol and distilled water. Finally, the product was recrystallized from petroleum ether to obtain the pure compound.

3-(4-bromobenzyl)-2-mercaptoquinazolin-4(3H)-one (B)

Off-white solid; Chemical formula $C_{15}H_{11}N_2OSBr$; yield: 80%; m.p. 216–218°C conducting a literature survey [24] ;R_f=0.637 ; FT-IR (υ, cm^{-1}): 3377 (N-H) ; 2941,2864(C-H aliphatic); 1664(C=O quinazolinone) ; 1577 (C=N); 1541,1515 (C=C aromatic) ; 808 (C-Br); ^{1}H-NMR:(H, ppm): 4.52 (s, 2H, N-CH_2), 6.6-8.4 (m, 8H, Ar-H), 11.2(s, 1H ,SH).^{13}C-NMR (C, ppm): 45.65 (N-CH_2), 110.1-139- (Ar-C), 151.14(C=N quinazolinone), 169.7 (C=O quinazolinone).

2.3 *Preparation of Specimens*

Meticulous preparation was essential for fabricating the carbon steel 45 artificial electrode. The electrode's chemical composition (wt%) was a critical factor and is detailed in Table1 [25]. Each electrode for the experimental trials was precisely cut into 2 × 2 × 0.1 cm pieces to ensure accuracy and consistency. To achieve optimal surface quality, a multi-step preparation process was followed. This involved progressive polishing using eight grades of emery paper, ranging in grit size from 150 to 2000. This range of abrasiveness ensured meticulous surface preparation, achieving the desired smoothness and texture. After

polishing, the electrodes were cleaned thoroughly in two steps. First, they were washed twice with acetone to remove any debris or contaminants that could compromise the accuracy of the tests. Second, the electrodes were rinsed with double-distilled water to eliminate any residual acetone, ensuring a clean and uncontaminated surface [26].

Table 1: Chemical composition of carbon steel C45

Metal	C%	S%	Mn%	S%	P%	Cu%	Ni%	Cr%	Fe%
Carbon Steel 45	0.36-0.42	0.15-0.30	1.00-1.40	0.05	0.05	0.50	0.20	0.20	96.88-97.49

2.4. *preparation of inhibitor Solutions*

Solutions with concentration of 0.01, 0.05, 0.1 and 0.3 M were prepared by dissolving (B) 3-(4-bromobenzyl)-2-mercaptoquinazolin-4(3H)-one in 1 M HCl. The corrosion system setup, including the electrochemical cell, is shown in Figure 1.

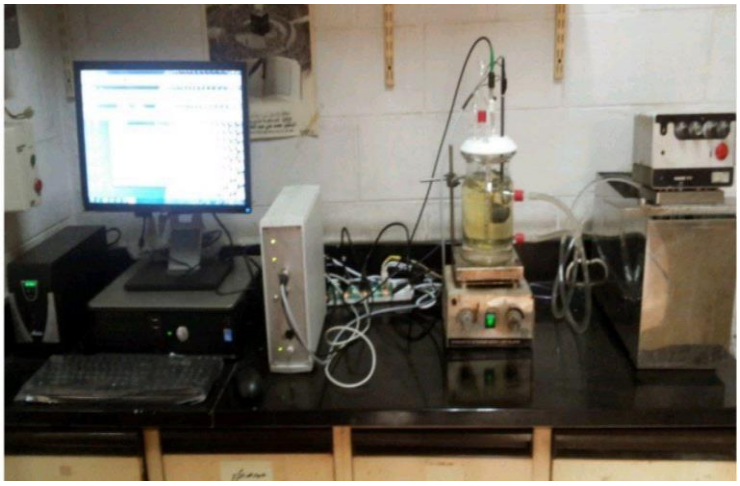

Figure 1: Potential-state system.

3. Results and Discussion

3.1 *Chemistry*

A novel 3-(4-bromobenzyl)-2-mercaptoquinazolin-4(3H)-one (B) as agent that inhibit the corrosion process. In this study produced heterocyclic compound containing nitrogen, sulfur, and oxygen atoms, as well as the compound (B) shown in Scheme (1). the reaction of anthranilic acid with a thiocyanate derivative (*P*-bromo benzyl thiocyanate) to produce 3-(4-bromobenzyl)-2-mercaptoquinazolin-4(3H)-one (B). FT-IR spectral data for compound (B) showed the disappearance of the NH_2 peak and the appearance of a single peak belonging to NH at 3377 cm^{-1}. Due to the presence of tautomerism C=S and C=N bonds. A weak peak also appears at 2563 cm^{-1} for SH. Also, the C=O peak appeared at 1664 cm^{-1} and a peak appeared at 1577 for C=N [24]. The C-Br is appeared at 808 cm^{-1}. ^{1}H-NMR spectroscopy for compound (B) shows a single peak at 4.5ppm belonging to CH_2, while the SH peak appears at 11.2ppm. The ^{13}C-NMR spectra for compound (B) showed the appearance of a peak at 45.6ppm belonging to CH_2 and 169ppm belonging to C=O, while the peak 151.14ppm belongs to C-SH [27]. The spectral diagnosis applies to the selection of compound B in tautomerism because the electronegativity of nitrogen is higher than that of sulfur and it is difficult to extract a proton from it, and this shape gives more stability to the compound. Scheme 2 shows the mechanisms of reaction.

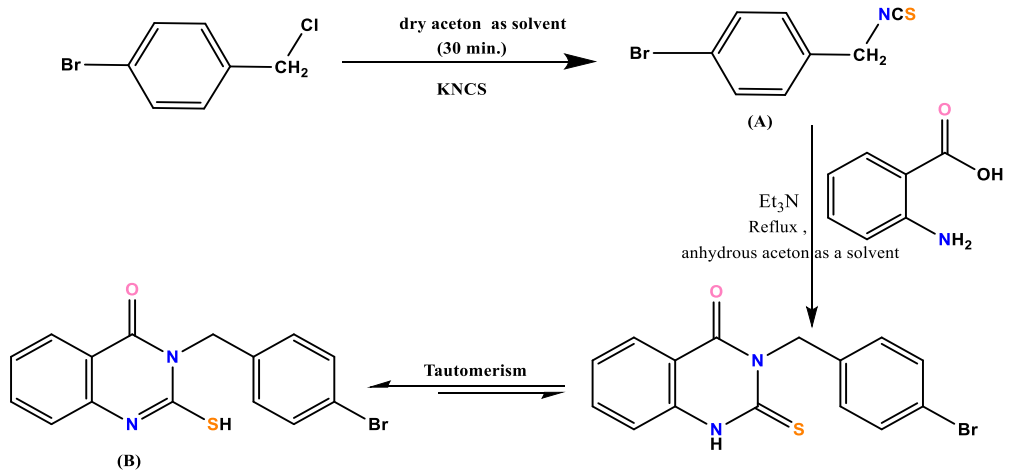

Scheme 1: Synthesis of 3-(4-bromobenzyl)-2-mercaptoquinazolin-4(3H)-one (B).

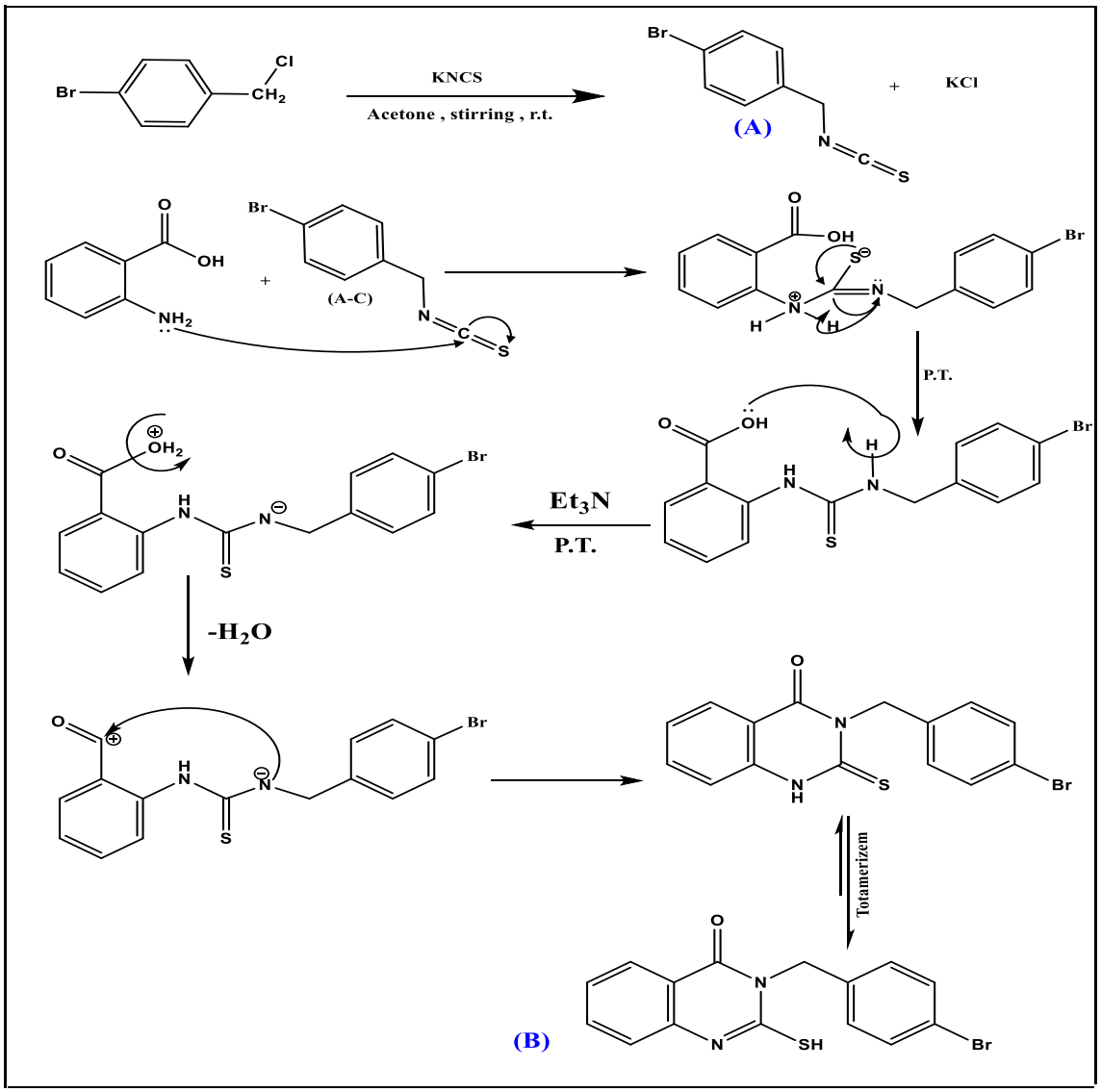

Scheme 2:Mechanisms of synthesis for compound 3-(4-bromobenzyl)-2-mercaptoquinazolin-4(3H)-one (B).

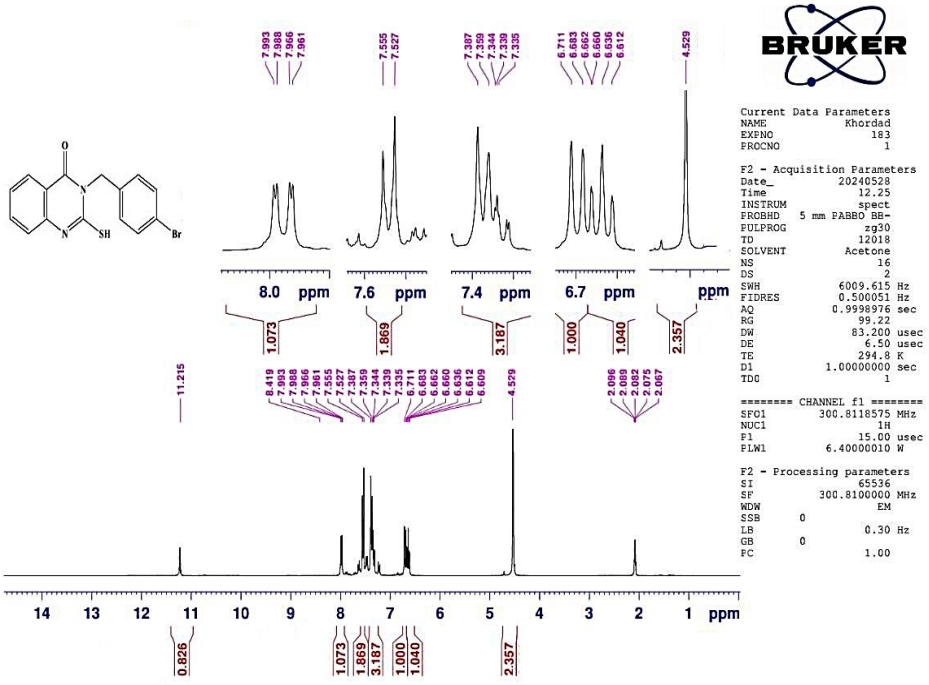

Figure 2: ^{1}H-NMR for compound (B)

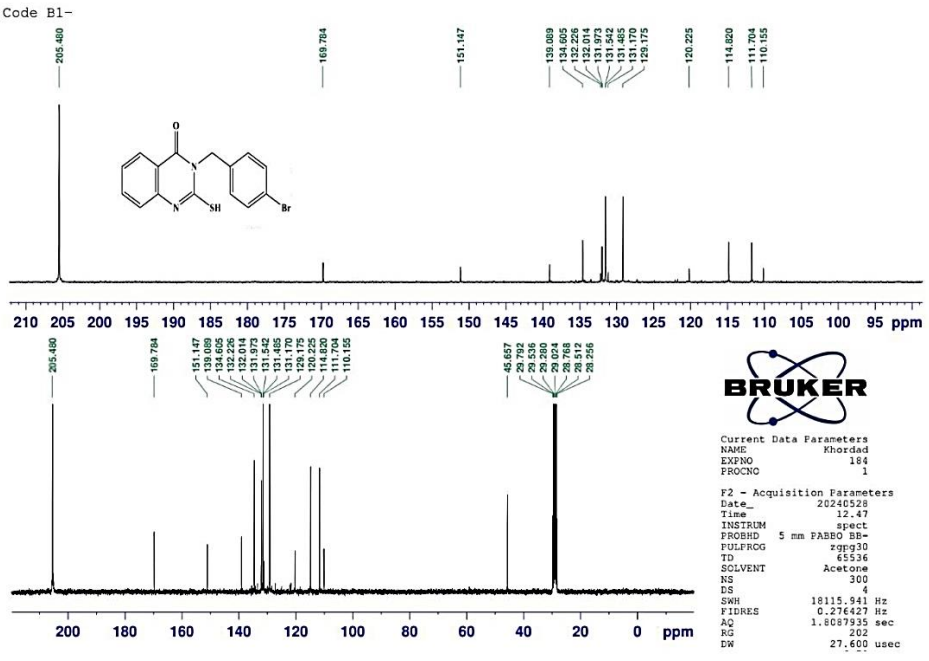

Figure 3: ^{13}C-NMR for compound (B).

3.2 *Study of potentiostatic polarization*

Following surface polishing, the electrode potential was stabilized at open circuit potential (OCP) for 15 minutes prior to Tafel polarization testing. The potential was systematically adjusted, and polarization curves were recorded automatically within a range of -200 mV to +200 mV vs. OCP at a scan rate of 2.0 mV/s. The open-circuit potential was used to calculate

the range of the curve. The temperatures used in each experiment were 293, 303, and 313 K. The corrosion potential (Ecorr) and corrosion current density (Icorr) were calculated at concentrations of 0.01M, 0.05M, 0.1M, and 0.3M, both in the presence and absence of an inhibitor. Lines representing potential versus Icorr were displayed on a logarithmic scale [28] .

3.3 *Polarization measurements*

The corrosion of carbon steel in a 1 M HCl solution at various temperatures was investigated using potentio-static polarization curves, both with and without the newly produced derivative (B). Figure 4 illustrates the behavior of the solution with and without the inhibitor (B) at temperatures of 293, 303, and 313 K. A linear relationship, represented by the Tafel slope, was observed. As previously mentioned, the cathodic reaction was inhibited by combining the sample examined in both the anodic and cathodic potential domains, resulting in a decrease in current density. These results suggest that the studied inhibitor most likely exhibits mixed inhibition behavior. Interestingly, when this inhibitor was used, the corrosion potential did not change, indicating that both anodic and cathodic processes were inhibited. The electrochemical parameter values are shown in Table 2, despite minor differences in potential due to competition between these processes. The corrosion system consists of a temperature-regulating device and three main electrodes. The reference electrode is a combination of two tubes, where the inner tube contains Hg/Hg_2Cl_2 (saturated KCl) and is used to determine the potential of the working electrode based on the potential of the reference electrode. The second electrode, known as the auxiliary electrode, consists of a 10 cm long high-purity platinum wire. The third electrode is the working electrode, whose potential should be measured and is represented by a metal wire connected to the sample. Figure 1 shows the potentio-static system setup.

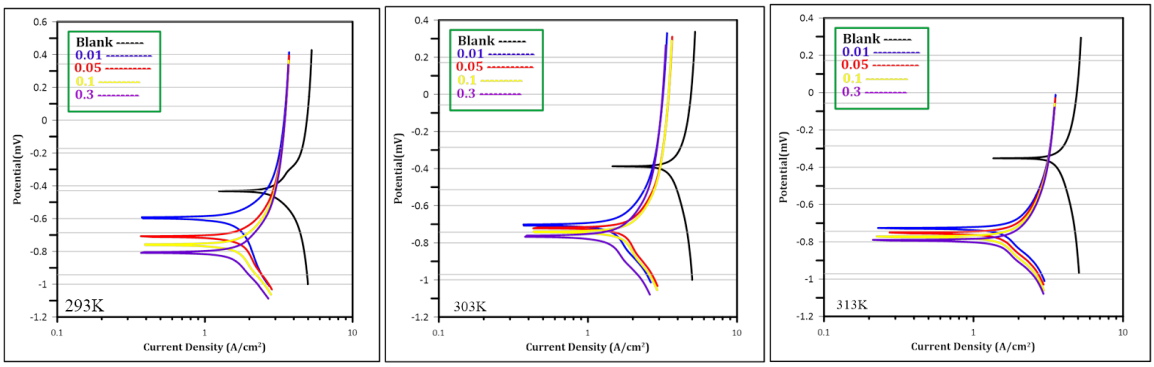

Figure 4: Polarization curves for corrosion of compound B+blank in HCl (1)

Table 2: Corrosion parameters for compound B and blank in HCl(1M) for different concentrations and temperatures.

Comp.	Blank	0.01	0.05	0.1	0.3	Blank	0.01	0.05	0.1	0.3	blank	0.01	0.05	0.1	0.3
Temp.	**293**					**303**					**313**				
-Ecorr (mV)	-0.427	-0.582	-0.661	-0.689	-0.737	-0.385	-0.770	-0.757	-0.742	-0.720	-0.385	-0.750	-0.759	-0.735	-0.716
Icorr (μA/cm²)	493.9	23.60	22.78	20.79	18.76	563.2	44.92	42.45	37.90	32.18	794.5	53.97	46.47	41.85	38.83
I corr./r (A/cm²)	9.878E-4	4.720E-5	4.556E-5	4.159E-5	3.752E-5	0.001	4.492E-5	8.489E-5	7.581E-5	3.218E-5	0.002	1.079E-4	9.293E-5	8.370E-5	7.766E-5
Resis. (Ω)	70.31	2394	2012	2232	2572	28.96	1582	1700	1773	1847	30.41	1182	1283	1336	1355
-Bc (mV/Dec)	0.156	0.177	0.153	0.163	0.209	0.055	0.362	0.334	0.301	0.245	0.087	0.342	0.326	0.279	0.236
Ba (mV/Dec)	0.164	0.488	0.342	0.310	0.237	0.120	0.299	0.331	0.318	0.310	0.154	0.257	0.237	0.239	0.249
Corr. rate, (mm/y)	4.848	0.232	0.224	0.204	0.184	5.529	0.220	0.417	0.372	0.158	7.799	0.530	0.456	0.411	0.381
IE%	**-**	**95**	**95**	**96**	**96**	**-**	**92**	**92**	**93**	**94**	**-**	**93**	**94**	**94**	**95**

(E corrosion, mV ,I corrosion, μA/cm^2); I corrosion per surface area(A/cm²) Polarization Resistance(Ω); Anodic β Tafel constant(mV/decade); Cathodic β Tafel constant(mV/decade); Corrosion rate(mm/year); IE% Inhibition-Efficiency

Tables 2 and Figure 4 present the results of the evaluation of the corrosion parameters. By extrapolating the cathodic and anodic Tafel curves in the presence and absence of the inhibitor molecules in a 1 M HCl solution, the corrosion potential (E_{corr}) and corrosion current density (I_{corr}) were determined. The resulting data in Table 2 and Figure 4 include the corrosion potential (E_{corr}, mV), corrosion current density (I_{corr}, A/cm²), cathodic and anodic Tafel slopes (mV/dec), and protection efficiency (PE%) were also used to compute the anodic (b_a) and cathodic (b_c) tafel slopes [29]. The Tafel slope refers to the gradient of the linear portion of the Tafel plot, which is generated by plotting the logarithm of the current density ($\log I_{corr}$) against the potential (E) in electrochemical studies. This slope provides insight into the kinetics of electrochemical reactions, specifically the rates of oxidation or reduction (anodic or cathodic reactions) taking place at the electrode surface.

Table 2 presents the values of the cathodic polarization slopes (b_c) and the anodic polarization slopes (b_a). The addition of an inhibitor results in changes to both the anodic and cathodic reactions. Higher values of b_c and b_a indicate a reduced rate of corrosion. Since the inhibitor influences both pathways of these reactions. This suggests that the inhibitor exhibits mixed-type behavior.

$$\%IE = \frac{(icorr)o-(icorr)}{(icorr)o} * 100 \quad (1)$$

Where $(i_{corr})_o$is the corrosion current density in the absence of inhibitor, (i_{corr}) is the corrosion current density in the presence of inhibitors .

3.4 *The effect of inhibitor concentration and Temperature*

Lower current densities signify improved corrosion inhibition, reflecting decreased corrosion rates. Conversely, as the temperature increases (293K → 313K), the current density generally rises for the blank (no inhibitor), indicating higher corrosion rates at elevated temperatures without an inhibitor. Based on the data, the best condition for corrosion inhibition is achieved with a 0.3M inhibitor concentration at 293K, as it results in the lowest current density and the highest level of corrosion protection, as shown in Figure 5.

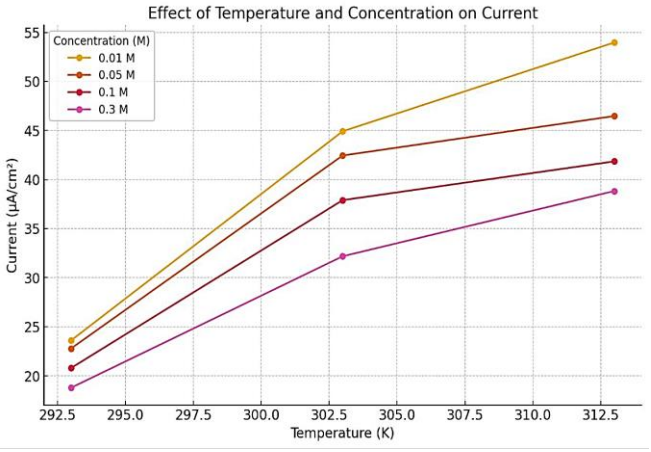

Figure 5: Relationship between inhibitor [B] inhibition currents for carbon steel in HCl(1M) at different concentrations(0.01,0.05,0.1 and 0.3M) and Temperatures(293,303 and 313K).

High inhibition efficiency occurs when the current density is lower. This can be explained as follows:

1. Increase in Current Density with Increasing Temperature:

A. Thermal Activation: As the temperature increases, the kinetic energy of the particles in the system also increases. This enhances the rate of electrochemical reactions because more molecules acquire sufficient energy to overcome the activation barrier.

B. Faster Reactions: Higher temperatures accelerate both oxidation and reduction reactions at the electrode surface, resulting in an increased reaction rate.

C. Increased Charge Transfer: The higher reaction rates lead to increased charge transfer at the electrode surface, which causes a rise in current density.

Therefore, at elevated temperatures, electrochemical reactions become more efficient, leading to higher current densities.

2. Decrease in Current Density with Increasing Inhibitor Concentration:

A. Inhibition of Reaction Sites: Inhibitors slow down or block electrochemical reactions. At higher concentrations, inhibitors bind to the active sites on the electrode surface or interact with reactive species in the solution, reducing the overall reaction rate.

B. Reduced Availability of Active Sites: The inhibitor physically or chemically blocks active sites on the electrode or interferes with the reactive species, resulting in fewer reactions at the electrode surface.

C. Lower Current Density: With fewer reactions occurring, the rate of charge transfer decreases, resulting in a reduction in current density.

The inhibition efficiencies at 293 K are quite closer, even with different concentrations. This is due to the fact that the calculated inhibition efficiencies are based on the change in inhibition current, which is relatively small. As a result, the values for inhibition efficiency remain close to each other.

3.5 *Adsorption Isotherms*

Adsorption isotherms are essential for understanding the interactions between inhibitors and metal surfaces. In this context, a possible adsorption mechanism involves substitutional

adsorption, where organic molecules in the aqueous solution (Org(sol)) displace water molecules previously adsorbed on the metal surface (H_2O(ads)) at the metal-solution interface [30].

$$Org\ (sol) + x\ H_2O\ (ads) = Org\ (ads) + xH_2O\ (sol) \quad (2)$$

Where: H_2O(ads) is the water molecule adsorbed on the metallic surface. Org(sol) and Org(ads) are the organic species in the bulk solution and on the metallic surface, respectively. x is the size ratio, indicating the number of water molecules replaced by one organic adsorbate. To determine the adsorption isotherm, Equation (3-A) was used to calculate the degree of surface coverage (Θ) for a variety of inhibitor dosages dissolved in a 1 M HCl solution. Table 3 presents the values of Θ. According to Langmuir's isotherm, the following equation links the inhibitor concentration (C) to the surface coverage (Θ) [31].

$$C/\Theta = 1/ K_{ads} + C \quad (3\text{-A})$$

Where: K_{ads} is the equilibrium constant for the inhibitor adsorption process. Figure 6 shows the plot of C/Θ versus C, which results in a straight line. The coefficient of linear correlation (R^2) is nearly equal to 1, and the slope is very close to 1, indicating that the adsorption of the synthetic inhibitor (B) on the surface of carbon steel follows the Langmuir adsorption isotherm. The Plot C/Θ vs. C: using data for various inhibitor concentrations (C) and corresponding surface coverages (Θ), plot C/Θ on the y-axis against C on the x-axis. If the data fits the Langmuir isotherm model, the plot should produce a straight line with a slope of 1 and an intercept of $1/K_{ads}$. Calculate K_{ads}: From the plot, the slope of the line should be 1, and the intercept should be $1/K_{ads}$. The value of K_{ads} can be determined from the intercept Equation(3-B):

$$K_{ads} = 1/ \text{Intercept of the plot} \quad (3\text{-B})$$

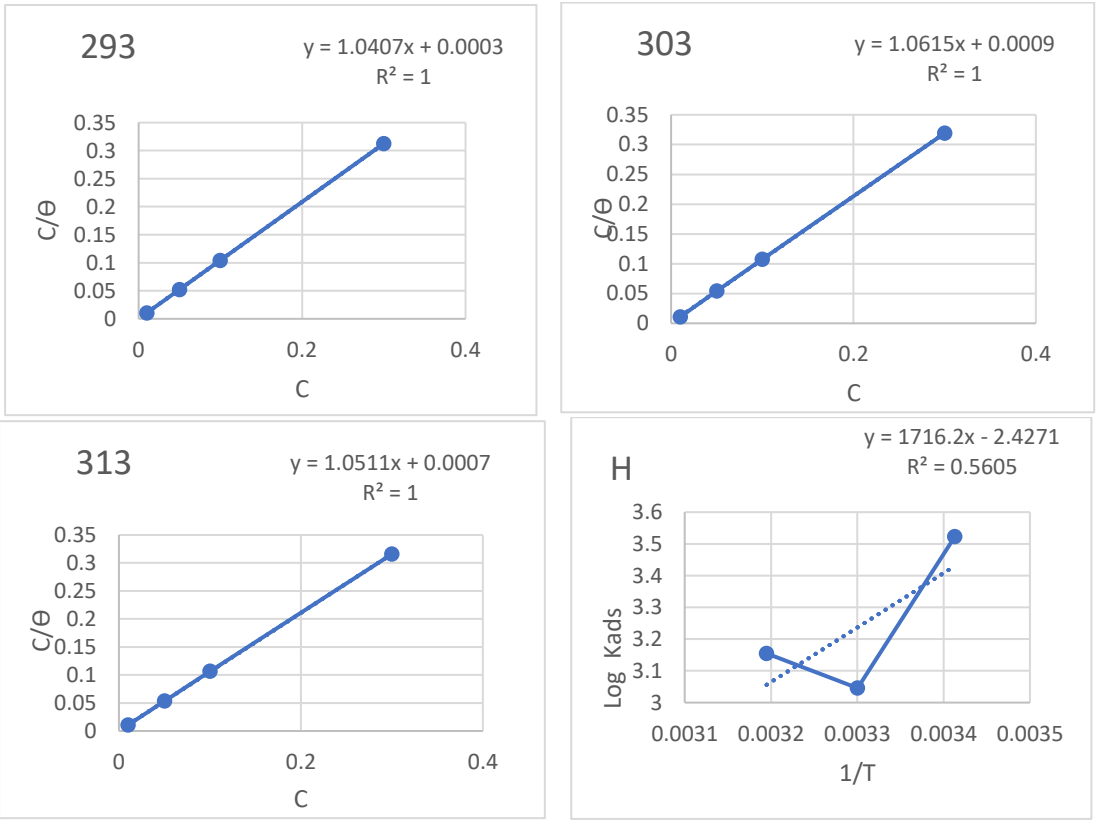

Figure 6: The Langmuir isotherm adsorption for carbon steel in 1M HCl at varied doses of inhibitor (B) at (293,303,313) K**.**

H: graph show the liner relationship between Log K_{ads} vs. 1/T to calculating ΔH_{ads}..

Table 3: The degree of surface coverage and the parameter of the adsorption isotherm for carbon steel in (1M) HCl at varying doses of inhibitor (B) at (293,303 and 313) K **.**

T(K)	1/T(K^{-1})	C(M)	Ɵ	C/ Ɵ	K_{ads}(M^{-1})	R^2
293	0.00341	0.01	0.95	0.01052	3333.33	1
		0.05	0.95	0.05263		
		0.1	0.96	0.1041		
		0.3	0.96	0.3125		
303	0.00330	0.01	0.92	0.01086	1111.11	1
		0.05	0.92	0.05434		
		0.1	0.93	0.1075		
		0.3	0.94	0.3191		
313	0.00319	0.01	0.93	0.01075	1428.57	1
		0.05	0.94	0.05319		
		0.1	0.94	0.10638		
		0.3	0.95	0.31578		

The strong correlation (R^2) observed in The Langmuir adsorption equation demonstrates the effectiveness of the mechanism by which the inhibitor adsorbs onto surfaces. The reciprocal of the intercept can be used to calculate the equilibrium constant (K_{ads}) for the inhibitor's adsorption-desorption process. Table 3 presents the results derived from the data, including the values of the adsorptive equilibrium constant (K_{ads}). Additionally, the information in Table 3 shows that the adsorptive equilibrium constant (K_{ads}) increased slightly with temperature, as the values were observed to rise between 293 K, 303 K, and 313 K [32]. A higher value of K_{ads} indicates stronger adsorption of the inhibitor onto the metal surface, implying better inhibition.

Research on dynamic polarization has demonstrated that the nitrogen-containing inhibitor affects the electrochemical reaction rather than neutralizing the acidity of hydrochloric acid, as the pH value did not significantly change upon the addition of the inhibitor to the hydrochloric acid medium. Additionally, Table 2 shows a minor shift in the E_{corr} values, with resistance rising and E_{corr} and I_{corr} declining. This implies that the inhibitor lowers the rate of corrosion by creating a barrier that slows down the rate of reaction. Furthermore, the data presented in Figure 6 and Table 3, along with the Langmuir adsorption model, support the conclusion that the inhibitor adsorbs onto the metal surface. This indicates that the substance does more than just operate as a base that lessens the effects of the acidic medium.

3.6 *Thermodynamic adsorption parameters*

The following formula was applied to the results obtained at different temperatures to determine the adsorption free energy (ΔG_{ads}):

$$\Delta G_{ads} = - 2.303\ RT \log (55.5\ K_{ads}) \quad (4)$$

Where: T is the absolute temperature in Kelvin, R is the gas constant, $K_a$ds is the equilibrium constant for the inhibitor adsorption. Table 4 presents the results of the thermodynamic analysis of the adsorption process. The enthalpy of adsorption (ΔH_{ads} =-32.86KJ/mol) falls within the typical range for physical adsorption, which is between (-10KJ/mol and -40KJ/mol) , indicating weak van der Waals forces between the adsorbate and the adsorbent. In contrast, chemical adsorption generally involves stronger bond formation

with enthalpy values exceeding -80KJ/mol [33]. The entropy change (-0.01137,-0.01686, and 0.01137KJ/mol.K) is small and negative, reflecting a slight decrease in randomness, which is common for physical adsorption where adsorbate molecules lose some freedom of movement on the adsorbent surface. In contrast, chemisorption often leads to more significant structural changes and a more pronounced negative entropy change [34]. The calculated Gibbs free energy (-29.53,-27.75 , and -29.30KJ/mol) values are all negative, confirming the spontaneity of the process. While both physical and chemical adsorption are spontaneous, the consistent negative Gibbs free energy values across different temperatures align more closely with chemical adsorption[35]. Together, the moderate enthalpy[36], small negative entropy change, and spontaneous Gibbs free energy indicate that the adsorption process is driven by forming coordination bonds, typical of chemical adsorption[37]. These thermodynamic parameters highlight the distinction between physical and chemical adsorption.

$$\Delta G_{ads} = \Delta H_{ads} - T\Delta S_{ads} \quad (5)$$

Table 4: Thermodynamic information for the adsorption inhibitor B on carbon steel in 1M HCl .

T (K)	ΔG_{ads} k J.mol^{-1}.K^{-1}	ΔH_{ads} kJ.mol^{-1}.	ΔS_{ads} KJ.mol^{-1}.K^{-1}
293	-29.53	-32.86008	-0.01137
303	-27.75		-0.01686
313	-29.30		-0.01137

3.7 *Activation Parameters*

A kinetic model is also employed in thermodynamics to describe the inhibition of corrosion. The Arrhenius equation is commonly used to model the corrosion reaction:

$$\text{Log Icorr} = \log A - Ea^*/2.303RT \quad (6)$$

Where: R is the fundamental gas constant, Icorr is the corrosion current density (a measure of the current flow), T is the absolute temperature, E_a* is the activation energy for the corrosion reaction, A is the Arrhenius pre-exponential factor. The Arrhenius equation provides a correlation between temperature and the reaction rate, helping to understand the energy barrier (activation energy) that needs to be overcome for corrosion to occur. The Arrhenius graphs in Figures 7 and 8, showing the relationship between the natural logarithm of the current density (log Icorr) and 1/T for various inhibitor concentrations (0.01, 0.05, 0.1, and 0.3 M) at different temperatures, illustrate this relationship for a 1 M solution of HCl. The relationship is described by Equation (6). Activation energy (E_a*) is the minimum energy needed for a chemical reaction, particularly in the context of corrosion reactions. According to the Arrhenius equation, a higher activation energy results in a lower corrosion rate. This indicates that the reaction occurs more slowly, which reflects better inhibition or increased resistance to corrosion (A higher activation energy (E_a*) value in this study indicates a lower rate of corrosion).

$K=Ae^{-Ea^*/RT}$ Arrhenius equation

The corrosion of the carbon steel surface is significantly reduced at 0.3 M inhibitor concentration, where the E_a* value is notably high [38]. The transition state equation (7) is used to compute the activation enthalpy (ΔH*) and activation entropy (ΔS*)[39].:

$$\text{Log Icorr} / T = (\log R/N\,Ah) + (\Delta S^*/2.303R) - (\Delta H^*/2.303RT) \quad (7)$$

R = universal gas constant ΔH*= activation enthalpy ΔS*= Activation entropy . h =Planck's constant NA = Avogadro's number.

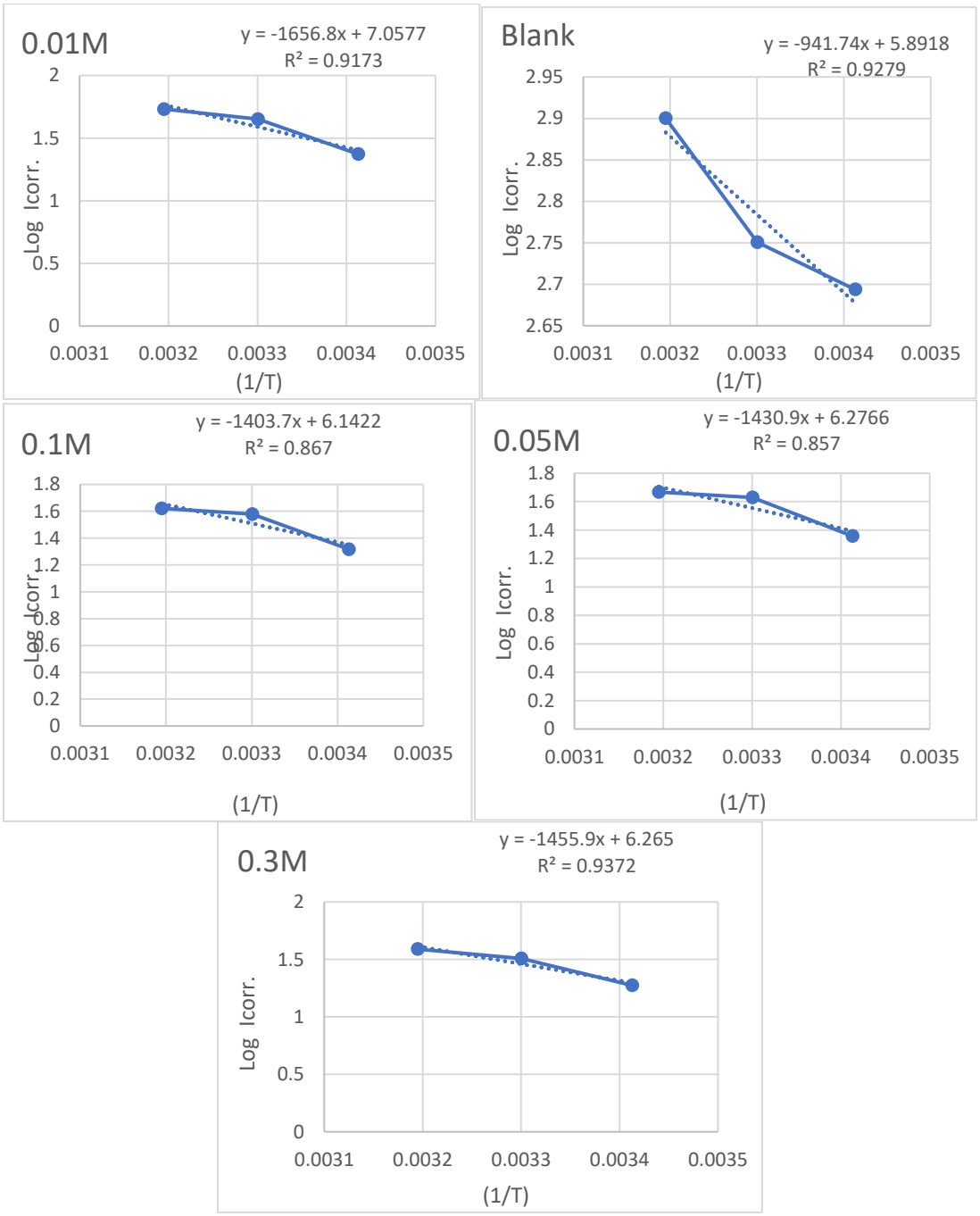

Figure 7: Plot of Log Icorr./T Vs.1/T for inhibitor 3-(4-bromobenzyl)-2-mercaptoquinazolin-4(3H)-one(B).

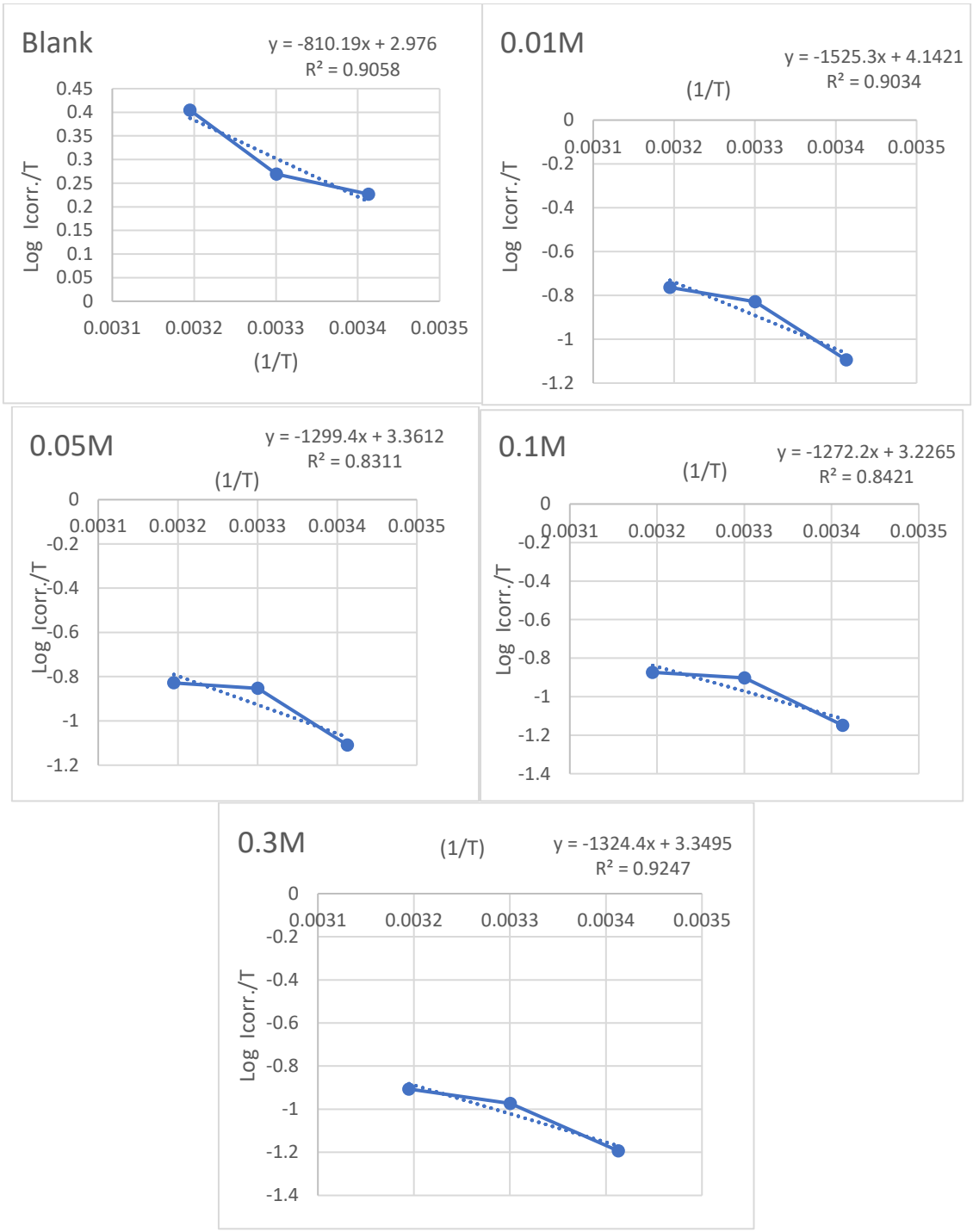

Figure 8: Arrhenius plots of log Icorr/T against 1/T in the presence and absence of derivatives at concentrations of 0.01M, 0.05M, 0.1M, and 0.3M, measured at a range of temperatures For Compound (B).

Table 5: The thermodynamic characteristics of the synthetic inhibitors' activation in 1M HCl For Compound (B)

Sample	T(K)	ΔE* KJ/mol	ΔH* KJ/mol	ΔS* J/mol.K	ΔG* KJ/mol.K
BLANK	293	18.0316295	15.56	-142.62	57.347
	303				58.774
	313				60.2001
0.01	293	31.72298	29.25	-120.87	64.665
	303				65.874
	313				67.082
0.05	293	27.39765	24.98	-133.46	64.084
	303				65.418
	313				66.753
0.1	293	26.8768	24.39	-136.74	64.455
	303				65.822
	313				67.1896
0.3	293	27.8763	25.37	-140.27	66.469
	303				67.872
	313				69.275

Conclusion

This study examined the corrosion inhibition performance of 3-(4-bromobenzyl)-2-mercaptoquinazolin-4(3H)-one, synthesized through a straightforward method with an 80% yield. Its effectiveness was evaluated using the potentiostatic technique. The findings demonstrated that the mercaptoquinazolinone derivative effectively inhibits corrosion of carbon steel (CS45) in acidic environments (1M HCl), achieving a peak inhibition efficiency of 96%. Adsorption studies showed that the compound follows Langmuir's adsorption isotherm, and thermodynamic analysis indicated that the adsorption process is chemosorption, based on the calculated enthalpy and free energy values. The compound exhibited strong corrosion inhibition effectiveness by significantly reducing the current density on the metal surface. It was observed that increasing the temperature led to higher current density due to accelerated electrochemical reactions, while increasing the inhibitor concentration effectively decreased the current density by blocking or hindering active corrosion sites. These findings highlight the potential of 3-(4-bromobenzyl)-2-mercaptoquinazolin-4(3H)-one as a reliable corrosion inhibitor for industrial applications in acidic conditions.

Recommendation

Researchers suggest to study various environments, such as sulfuric acid and sodium chloride saline solutions, in addition to preparing quinazolinone derivatives with different substituents.

References

[1] R. Yadav, and G. S. Pathak, "Young consumers' intention towards buying green products in a developing nation: Extending the theory of planned behavior," *Journal of cleaner production,* vol. 135, pp. 732-739, 2016.

[2] P. B. Matad, P. B. Mokshanatha, N. Hebbar, V. T. Venkatesha, and H. C. Tandon, "Ketosulfone drug as a green corrosion inhibitor for mild steel in acidic medium," *Industrial & Engineering Chemistry Research,* vol. 53, no. 20, pp. 8436-8444, 2014.

[3] I. Obot, D. Macdonald, and Z. Gasem, "Density functional theory (DFT) as a powerful tool for designing new organic corrosion inhibitors. Part 1: an overview," *Corrosion Science,* vol. 99, pp. 1-30, 2015.

[4] L. Yang, *Techniques for corrosion monitoring*: Woodhead Publishing, 2020.

[5] R. Touir, N. Errahmany, M. Rbaa, F. Benhiba, M. Doubi, E. E. Kafssaoui, and B. Lakhrissi, "Experimental and computational chemistry investigation of the molecular structures of new synthetic quinazolinone derivatives as acid corrosion inhibitors for mild steel," *Journal of Molecular Structure,* vol. 1303, pp. 137499, 2024.

[6] W. Ettahiri, R. Salim, M. Adardour, E. Ech-Chihbi, I. Yunusa, M. M. Alanazi, S. Lahmidi, A. E. Barnossi, O. Merzouki, and A. Iraqi Housseini, "Synthesis, characterization, antibacterial, antifungal and anticorrosion activities of 1, 2, 4-triazolo [1, 5-a] quinazolinone," *Molecules,* vol. 28, no. 14, pp. 5340, 2023.

[7] L. T. Popoola, A. O. Agbo, U. Taura, A. S. Yusuff, Y. P. Asmara, O. A. Olagunju, and O. M. Chima, "Weight loss and electrochemical measurements of aluminum corrosion in diesel fuel and biodiesel prepared via transesterification of waste cooking oil," *Results in Engineering,* vol. 24, pp. 103373, 2024.

[8] H. Malki, A. Ameziane Elhassani, S. El Hamzi, N. Dkhirech, I. Forsal, F. Elhajri, Z. Benzekri, A. Benjelloun, and S. Boukhris, "Investigating Quinazolinone Derivatives as Corrosion Inhibitors for Mild Steel in 1.0 M HCl: Experimental Insights, DFT Calculations, and MC Simulations," *Analytical and Bioanalytical Electrochemistry,* vol. 16, no. 6, pp. 568-594, 2024.

[9] W. N. Al-Sieadi, O. H. Al-Jeilawi, N. A. Khudhair, A. N. Shamaya, and N. A. Abdulrahman, "Synthesis and characterization of heterocyclic derivatives to evaluate their efficiency as corrosion inhibitors for carbon steel in saline medium," *Advanced Journal of Chemistry, Section A,* vol. 8, no. 2, pp. 209-219, 2025.

[10] Y. Qiang, S. Zhang, B. Tan, and S. Chen, "Evaluation of Ginkgo leaf extract as an eco-friendly corrosion inhibitor of X70 steel in HCl solution," *Corrosion Science,* vol. 133, pp. 6-16, 2018.

[11] M. Safi, L. Ahamed, and T. Hadda, "Synthesis and experimental study of new coumarin derivatives as corrosion inhibitors for carbon steel surfacein 3.5% NaCl," *International Journal of Corrosion and Scale Inhibition,* vol. 13, no. 4, pp. 2156-2179, 2024.

[12] J. Akpoborie, O. Fayomi, A. Inegbenebor, A. Ayoola, O. Dunlami, O. Samuel, and O. Agboola, "Electrochemical reaction of corrosion and its negative economic impact." p. 012071.

[13] Y. Qiang, S. Zhang, and L. Wang, "Understanding the adsorption and anticorrosive mechanism of DNA inhibitor for copper in sulfuric acid," *Applied Surface Science,* vol. 492, pp. 228-238, 2019.

[14] H. Li, Y. Qiang, W. Zhao, and S. Zhang, "2-Mercaptobenzimidazole-inbuilt metal-organic-frameworks modified graphene oxide towards intelligent and excellent anti-corrosion coating," *Corrosion Science,* vol. 191, pp. 109715, 2021.

[15] M. H. Sliem, M. Afifi, A. Bahgat Radwan, E. M. Fayyad, M. F. Shibl, F. E.-T. Heakal, and A. M. Abdullah, "AEO7 surfactant as an eco-friendly corrosion inhibitor for carbon steel in HCl solution," *Scientific reports,* vol. 9, no. 1, pp. 2319, 2019.

[16] R. M. Kubba, M. A. Mohammed, and L. S. Ahamed, "DFT calculations and experimental study to inhibit carbon steel corrosion in saline solution by quinoline-2-one derivative: Carbon steel corrosion," *Baghdad Science Journal,* vol. 18, no. 1, pp. 0113-0113, 2021.

[17] N. J. Maduelosi, and N. B. Iroha, "Insight into the adsorption and inhibitive effect of spironolactone drug on C38 carbon steel corrosion in hydrochloric acid environment," *Journal of Bio-and Tribo-Corrosion,* vol. 7, no. 1, pp. 6, 2021.

[18] N. M. Hashim, A. A. Rahim, H. Osman, and P. B. Raja, "Quinazolinone compounds as corrosion inhibitors for mild steel in sulfuric acid medium," *Chemical Engineering Communications,* vol. 199, no. 6, pp. 751-766, 2012.

[19] B. K. Raja, A. Philips, S. Ravi, M. Ravi, A. S. Palakkal, R. S. Pillai, and G. C. Senadi, "3-Phenylquinazolin-4 (3H)-one via a renewable approach as an efficient corrosion inhibitor for mild steel in acid media," *Materials Chemistry and Physics,* vol. 308, pp. 128238, 2023.

[20] Z. J. Witczak, "Monosaccharide isothiocyanates and thiocyanates: synthesis, chemistry, and preparative applications," *Advances in carbohydrate chemistry and biochemistry,* vol. 44, pp. 91-145, 1987.

[21] B. Maeda, and K. Murakami, "Recent advancement in the synthesis of isothiocyanates," *Chemical Communications,* vol. 60, no. 21, pp. 2839-2864, 2024.

[22] R. Alshehry, "Synthetic studies toward biologically active quinazolinones: a dissertation in Chemistry and Biochemistry," *University of Massachusetts Dartmouth*, 2022.

[23] A. Nasli Esfahani, A. Iraji, A. Alamir, S. Moradi, M. S. Asgari, S. Hosseini, S. Mojtabavi, E. Nasli-Esfahani, M. A. Faramarzi, and F. Bandarian, "Design and synthesis of phenoxymethybenzoimidazole incorporating different aryl thiazole-triazole acetamide derivatives as α-glycosidase inhibitors," *Molecular Diversity,* vol. 26, no. 4, pp. 1995-2009, 2022.

[24] P. S. Satpanthi, Trivedi, J. P., "Quinazolines. III. Synthesis of 2-alkyl-3-aralkyl-4-(3H)- and 2-mercapto-3-aralkyl(alkyl)-4(3H)-quinazolinones," *Journal of the Indian Chemical Society,* vol. 48, no. 11, pp. 1021-6, 1971.

[25] N. Ashwini, R. Dileep, and S. Ranganatha, "Quantum Chemical and Experimental Evaluation of a Curcumin Based Schiff Base as an Efficient Corrosion Inhibitor for Steel Material," *Materials Today Communications*, 2024.

[26] R. Mohammed, and S. Hussein, "Corrosion inhibition of carbon steel in saline water using an azo dye at various concentrations," *International Journal of Corrosion and Scale Inhibition,* vol. 13, no. 1, pp. 241-253, 2024.

[27] R. M. Silverstein, and G. C. Bassler, "Spectrometric identification of organic compounds," *Journal of Chemical Education,* vol. 39, no. 11, pp. 546, 1962.

[28] H. Almashhadani, "Using expired pharmaceutical Clotrimazole as a corrosion inhibitor for stainless steel in acidic media," *International Journal of Corrosion and Scale Inhibition,* vol. 13, no. 3, pp. 1636-1648, 2024.

[29] G. Mubarak, C. Verma, M. A. Mazumder, I. Barsoum, and A. Alfantazi, "Corrosion inhibition of P110 carbon steel useful for casing and tubing applications in 3.5% NaCl solution using quaternary ammonium-based copolymers," *Journal of Molecular Liquids,* vol. 402, pp. 124691, 2024.

[30] S. O. Adejo, T. Uzah, and J. Akuhwa, "Adsorption Isotherm Modeling in Corrosion Inhibition Studies," *Corrosion Engineering-Recent Breakthroughs and Innovative Solutions*: IntechOpen, 2024.

[31] H. Abubakar, A. Abubakar, and Z. Nasir, "Adsorption Isotherm Analysis of Black Seed (Nigella Sativa L.) Oil as an Eco-friendly Corrosion Inhibitor for Mild Steel in Acidic Environment," *Journal of Applied Sciences and Environmental Management,* vol. 28, no. 10B Supplementary, pp. 3493-3499, 2024.

[32] R. Mohammed, and H. Almashhadani, "Synthesis, characterization and thermodynamic study of a polymer nanocomposite from methyl acrylate and zirconium chloride as an anti-corrosion coating for carbon steel," *International Journal of Corrosion and Scale Inhibition,* vol. 12, no. 3, pp. 1180-1191, 2023.

[33] S. Sharma, R. Ganjoo, S. Kr. Saha, N. Kang, A. Thakur, H. Assad, V. Sharma, and A. Kumar, "Experimental and theoretical analysis of baclofen as a potential corrosion inhibitor for mild steel surface in HCl medium," *Journal of Adhesion Science and Technology,* vol. 36, no. 19, pp. 2067-2092, 2022.

[34] H. M. Elabbasy, and S. E. Aziz Abd Fouda, "Inhibitive behavior of Ambrosia Maritima extract as an eco-friendly corrosion inhibitor for carbon steel in 1M HCI," *Zastita Materijala,* vol. 60, no. 2, pp. 129-146, 2019.

[35] J. R. Smith, *Theory of chemisorption*: Springer Science & Business Media, **2013**.

[36] Sheetal, R. Batra, A. K. Singh, M. Singh, S. Thakur, B. Pani, and S. Kaya, "Advancement of corrosion inhibitor system through N-heterocyclic compounds: a review," *Corrosion Engineering, Science and Technology,* vol. 58, no. 1, pp. 73-101, 2023.

[37] N. Errahmany, M. Rbaa, A. S. Abousalem, A. Tazouti, M. Galai, E. H. E. Kafssaoui, M. E. Touhami, B. Lakhrissi, and R. Touir, "Experimental, DFT calculations and MC simulations concept of novel quinazolinone derivatives as corrosion inhibitor for mild steel in 1.0 M HCl medium," *Journal of Molecular Liquids,* vol. 312, pp. 113413, 2020/08/15/, 2020.

[38] Z. Aribou, M. Ouakki, F. El Hajri, E. Ech-Chihbi, I. Saber, Z. Benzekri, S. Boukhris, M. K. Al-Sadoon, M. Galai, and J. Charafeddine, "Comprehensive assessment of the corrosion inhibition properties of quinazoline derivatives on mild steel in 1.0 M HCl solution: An electrochemical, surface analysis, and computational study," *International Journal of Electrochemical Science,* vol. 19, no. 11, pp. 100788, 2024.

[39] A. I. Ikeuba, J. E. Ntibi, P. C. Okafor, B. I. Ita, A. U. Agobi, F. C. Asogwa, B. J. Omang, E. A. Eno, H. Loius, and S. A. Adalikwu, "Kinetic and thermodynamic evaluation of azithromycin as a green corrosion inhibitor during acid cleaning process of mild steel using an experimental and theoretical approach," *Results in Chemistry,* vol. 5, pp. 100909, 2023.